OSSE Observations of GX 339−4

D. A. Grabelsky, S. M. Matz, W. R. Purcell, and M. P. Ulmer
Department of Physics and Astronomy, Northwestern University, Evanston, IL 60208

J. E. Grove, W. N. Johnson, R. L. Kinzer, J. D. Kurfess, and
M. S. Strickman
E. O. Hulburt Center for Space Research, Code 7650, Naval Research Laboratory,
Washington, DC 20375

and

G. V. Jung
Universities Space Research Association, Washington, DC 20024

Accepted for publication in the Astrophysical Journal

ABSTRACT

The Oriented Scintillation Spectrometer Experiment on the *Compton Gamma Ray Observatory* observed the Galactic black hole candidate GX 339−4 as a target of opportunity in 1991 September, in response to the outburst reported by BATSE. We report here on energy spectra in the 50 keV to 10 MeV range obtained by OSSE. The source was detected from 50 to 400 keV at a level relative to the Crab nebula of $\sim 30\%$. The observed spectrum was described reasonably well by a power law with an exponential cutoff; a least-squares fit yielded a photon index of $.88 \pm .05$ and a cutoff energy of (68 ± 2) keV. The addition of a Compton reflection component did not significantly improve the overall fit. An optically-thin thermal bremsstrahlung spectrum also provides a good fit, and the thermal Comptonization model of Sunyaev and Titarchuk, while deficient in describing the data above about 200 keV, cannot formally be ruled out. A pure power law with reflection does not fit the observed spectrum. During a follow-up observation made in 1991 November, the intensity of the source below 100 keV

Report Documentation Page						*Form Approved* *OMB No. 0704-0188*
Public reporting burden for the collection of information is estimated to average 1 hour per response, including the time for reviewing instructions, searching existing data sources, gathering and maintaining the data needed, and completing and reviewing the collection of information. Send comments regarding this burden estimate or any other aspect of this collection of information, including suggestions for reducing this burden, to Washington Headquarters Services, Directorate for Information Operations and Reports, 1215 Jefferson Davis Highway, Suite 1204, Arlington VA 22202-4302. Respondents should be aware that notwithstanding any other provision of law, no person shall be subject to a penalty for failing to comply with a collection of information if it does not display a currently valid OMB control number.						
1. REPORT DATE **1995**		2. REPORT TYPE				3. DATES COVERED **00-00-1995 to 00-00-1995**
4. TITLE AND SUBTITLE **OSSE Observations of GX 339-4**						5a. CONTRACT NUMBER
						5b. GRANT NUMBER
						5c. PROGRAM ELEMENT NUMBER
6. AUTHOR(S)						5d. PROJECT NUMBER
						5e. TASK NUMBER
						5f. WORK UNIT NUMBER
7. PERFORMING ORGANIZATION NAME(S) AND ADDRESS(ES) **Naval Research Laboratory,Code 7650,4555 Overlook Avenue, SW,Washington,DC,20375**						8. PERFORMING ORGANIZATION REPORT NUMBER
9. SPONSORING/MONITORING AGENCY NAME(S) AND ADDRESS(ES)						10. SPONSOR/MONITOR'S ACRONYM(S)
						11. SPONSOR/MONITOR'S REPORT NUMBER(S)
12. DISTRIBUTION/AVAILABILITY STATEMENT **Approved for public release; distribution unlimited**						
13. SUPPLEMENTARY NOTES						
14. ABSTRACT						
15. SUBJECT TERMS						
16. SECURITY CLASSIFICATION OF:			17. LIMITATION OF ABSTRACT	18. NUMBER OF PAGES	19a. NAME OF RESPONSIBLE PERSON	
a. REPORT **unclassified**	b. ABSTRACT **unclassified**	c. THIS PAGE **unclassified**		**19**		

Standard Form 298 (Rev. 8-98)
Prescribed by ANSI Std Z39-18

had dropped by more than a factor of 40, and it was no longer detected above about 100 keV. The energy spectrum during the November observation could be characterized by a power law with a photon index of 2.3 ± 0.3; the spectrum was fit equally well with the same exponentially-cutoff power law model applied to the September observation, reduced in intensity by a factor of ~ 40. During the 1991 September observation, the luminosity in the 50–400 keV band was approximately 2×10^{37} ergs s^{-1} (assuming a distance of 4 kpc), no more than a factor of five below the soft X-ray luminosity of GX 339$-$4 observed in its X-ray high state. The luminosity during the 1991 November observation was $\sim 5 \times 10^{35}$ ergs s^{-1}. Extrapolations of both the exponentially-cutoff power law and Sunyaev-Titarchuk models to the ~5–20 keV X-ray band yield flux levels very close to that observed by GINGA during an overlapping interval in 1991 September, when GX 339$-$4 was reported to be in its low X-ray state. This may be one of the strongest indications to date of a direct correspondance between the low X-ray state and gamma-ray outbursts of GX 339$-$4.

Subject headings: stars: individual (GX 339$-$4) — X-rays: binaries — gamma-rays: general

1. INTRODUCTION

Galactic X-ray sources thought to be black hole candidates are usually characterized by extremely hard spectra, rapid and erratic time variability, and the occurrence of two or more longer time scale "states" of X-ray emission. Attribution of these properties to black holes rests in a large part on dynamical mass determinations of defining examples such as Cyg X-1 (Liang & Nolan 1984; Tanaka & Lewin 1994; and references therein). Even in the absence of well-established mass estimates, however, sources which exhibit this canonical behavior are of considerable interest to the study of accretion processes around compact objects. One of the best studied of these sources is GX 339$-$4. In X-rays it visits at least three states distinguished by their spectral and temporal properties. In the *high* or *soft* state, the soft X-ray flux is at its maximum, with a predominantly thermal spectrum and a relatively weak hard tail. The *low* or *hard* state exhibits a much lower soft X-ray flux, with a somewhat more luminous hard tail that extends to a few hundred keV, and rapid intensity variations. The *off* state is characterized by undetectable X-ray flux in the 2–10 keV range (Markert et al. 1973). Miyamoto et al. (1991), reporting on GINGA observations, found that GX 339$-$4 also exhibits a "very high state," with a soft X-ray flux 2–3 times the nominal high-state value and rapid time variability usually associated with the low state. Cowley, Crampton, &

Hutchings (1987) estimated a mass of $<2.5\ M_{\odot}$ for GX 339−4 from observations of emission lines assumed to arise in the disk. This conclusion is fairly uncertain, however, and GX 339−4 is still considered to be a possible black hole by virtue of its spectral and temporal behavior.

In 1991 August, BATSE reported a rapid increase of the gamma-ray flux from GX 339−4 (Fishman et al. 1991). In response, the Oriented Scintillation Spectrometer Experiment on the *Compton Gamma Ray Observatory* observed GX 339−4 as a target of opportunity beginning 1991 September 5. During this initial one-week observation, GX 339−4 was detected strongly by OSSE from 50 to 400 keV, at a level of approximately 300 mCrab. A second one-week observation was carried out beginning 1991 November 7, at which time GX 339−4 appeared to be about 40 times weaker at energies less than ~100 keV, and below the OSSE sensitivity at higher energies. The OSSE observations provide sensitive, high quality gamma-ray spectral measurements of GX 339−4. Preliminary results of the OSSE observations were reported by Grabelsky et al. (1993). In this paper we describe the observations and analysis of these data, and discuss our findings concerning the energy spectrum of GX 339−4 in the context of models for the emission from accreting compact objects.

2. OBSERVATIONS

The OSSE instrument consists of four separate, nearly identical NaI-CsI phoswich detectors sensitive to gamma-rays in the ~50 keV to 10 MeV range. Each detector has a tungsten slat collimator which defines an $3.8^{\circ} \times 11.4^{\circ}$ field of view (FWHM), and active shielding provided by NaI anti-coincidence detectors configured in an annulus around the main detector. The total geometric area of all four detectors is 2620 cm^2, and the photopeak effective area at 100 keV is 2000 cm^2. The detectors are mounted in pairs on two axes parallel to the long dimension of the collimator (also the y-direction of the spacecraft), and can independently rotate through 192° about these axes (i.e., in the spacecraft xz-plane). The independent positioning capability of the detectors is used for offset pointing for background estimation, and permits observation of a secondary target when the primary target is occulted by the earth. See Johnson et al. (1993) for a detailed description of the OSSE instrument and its operation.

The observations of GX 339−4 were carried out during 1991 September 5 – 12 and 1991 November 7 – 14. OSSE spectral observations consist of a series of alternating on- and off-source two-minute pointing cycles. The off-source pointings are used in post-observation data processing to estimate a background for each on-source pointing. During all of the observations of GX 339−4, the collimator was centered on the source ($l = 339^{\circ}$, $b = -4.3^{\circ}$)

with the long dimension oriented parallel to the Galactic plane. The on-source observing time during the unocculted portion of each orbit was shared equally between the binary X-ray source and a pointing in the Galactic plane at $l = 339°$, $b = 0°$. The off-source pointing positions were at $b = +4.5°$ and $-8.5°$; this allowed the same background pointings to be used for both source targets. The total on-source observing times (per detector) for the two observations were $\sim 5.7 \times 10^4$ s and $\sim 7.5 \times 10^4$ s, respectively. The spectral energy range covered 50 keV to 10 MeV. As described in the next section, the Galactic plane data were used to estimate the flux due to diffuse Galactic emission at the position of GX 339−4.

3. ANALYSIS AND RESULTS

The energy spectra were analyzed using the standard methods described in Johnson et al. (1993; see also Purcell et al. 1993). After routine data-quality screening, a background spectrum for each two-minute source pointing was estimated by fitting a quadratic to the nearest three or four two-minute background pointings. Each background estimate was subtracted from its associated on-source pointing, and the resulting background-subtracted source spectra were then summed on time scales of one day and one week (the duration of each viewing period). This procedure produced time-averaged count spectra for each detector during both observations. The observed count rate then consisted of emission from GX 339−4, as well as a diffuse component from the Galactic plane.

In order to determine the contribution of the diffuse Galactic emission, we fit a simple Gaussian latitude-distribution model to previous observations made as part of the OSSE Galactic plane survey. These data, centered at $l = 25°$, include out-of-plane pointings spaced symmetrically about $b = 0°$. A least-squares fit of the model latitude distribution, convolved with the OSSE collimator response in the 50–150 keV range, yielded a width (FWHM) of about 4 degrees. With the assumption that the same model (i.e., same FWHM) is valid at $l = 339°$, we used it to scale the observed count rate at $l = 339°$, $b = 0°$ to an expected level at $b = -4.3°$, taking into account exposure to the diffuse flux in the background positions. This expected count rate was then taken as the diffuse component at the position of GX 339−4, and subtracted from the "uncorrected" data; the correction was applied on the one-day and one-week time scales of the spectral sums. Because the in-plane observations at $l = 339°$ during both observing periods yielded consistent spectra (to within the uncertainties), the scaled data from the November observation alone were used in correcting both observations of GX 339−4.

The observed (uncorrected) count spectra summed over the respective week-long observations of GX 339−4 are shown in Figure 1, together with the estimated correction

spectrum due to the diffuse component. The spectra are displayed with no upper limits in this visual comparison, but it should be clear that beyond about 200 keV the significance of the data is only marginal at best (except for the September observation). For the November observation of GX 339−4, the relative contribution of the diffuse correction to the observed count rate varies from roughly 60% to 25% over the 50–150 keV band, with a level of $\sim$ 40% for the integral flux in this band. The contribution during the September observation is obviously negligible. All subsequent analysis discussed here has been applied to the corrected spectra.

Figure 2 shows integrated daily source intensities in the 50–100 keV and 100–400 keV bands, as well as the hardness ratio of these two bands, during the September observation. Although there appears to be a slight softening trend, the data are statistically consistent with a constant hardness ratio (χ^2 probability of $\sim$0.17 for a null result).

In the corresponding analysis of the average daily intensities for the November observation (not shown) the total average intensity in 50–100 keV band was 0.21 ± 0.05 counts s^{-1}, about a factor of 40 below the September value. The daily intensities in this band were consistent with the average during the November observation, but detected at no greater than the 3σ level. Only a marginally significant ($\lesssim 3\sigma$) signal was detected at energies $\gtrsim$ 120 keV.

The time-averaged spectra were fitted over the 0.05–1 MeV energy range using a forward-folding technique. The model photon spectrum was convolved with the OSSE instrument response to produce a model count spectrum, and the parameters of the input spectrum adjusted iteratively to minimize χ^2 of the fitted model count spectrum to the measured count spectrum. For a source as strong as GX 339−4 during the September observation, the statistical significance of the data is high enough that uncertainties in the OSSE instrument response and the precision of the cross calibration of the detectors become important. In order to evaluate the level of these effects, we fit the spectra from all four detectors individually, as well as simultaneously. For a given model, the fit results for each detector and for the combined four-detector data set were checked for consistency of the determined parameters. The fits were also compared on the basis of their χ^2 probabilities, i.e., the probability of obtaining by chance a χ^2 value greater than that observed, assuming the model is correct. Using the data from the September observation, the fitted parameter values were found to be statistically consistent among detectors for each of the models investigated here, and the χ^2 probabilities of the fits showed reasonable agreement among detectors as to the acceptability of each model. In the discussion below we report the parameters and χ^2 probabilities for the simultaneous, four-detector fits; Table 1 list our results.

The various models proposed for accreting stellar-mass black holes (as well as AGN)

generally include a component due to inverse Compton scattering of soft ($\sim$ a few keV) photons by a hot corona near the inner region of the accretion disk. The benchmark for discussing this class of models has been the thermal Comptonization model of Sunyaev & Titarchuk (1980), which assumes a large Thomson optical depth for the scattering cloud. For the case of a spherical corona, a fit to the OSSE spectrum observed in September yielded a temperature of kT = (37 $\pm$ 1) keV, and optical depth of τ = 3.0 $\pm$ 0.1, with a normalization at 100 keV of (0.189 ± 0.001) photons cm^{-2} s^{-1} MeV^{-1}. At energies below kT of the scattering medium the Sunyaev-Titarchuk spectrum is described by a power law with photon index given by $\alpha = -\frac{1}{2} + \sqrt{\frac{9}{4} + \gamma}$. Here $\gamma = \pi^2 mc^2/3kT(\tau + \frac{2}{3})^2$ is derived from the model parameters τ and kT, and gives the inverse of the average fractional energy gain of an emerging photon (i.e., the inverse of the Compton "y" parameter) for the assumed geometry (Sunyaev & Titarchuk 1980; see also Pozdnyakov, Sobol, & Sunyaev 1983). Our fit results thus correspond to α = 1.9 and γ = 3.4. While the model fits the OSSE data below about 200 keV, it cuts off much more rapidly than does the observed spectrum above this energy, giving the impression of a high-energy excess in the data. The χ^2 probability of 4×10^{-3} indicates that the fit is only marginal, at best.

In an analysis of archival EXOSAT observations of Cyg X-1, Haardt et al. (1993) suggested that optically thin Comptonization might be a more appropriate model for accreting black holes, and pointed out that such a spectrum is approximated well by a power law with an exponential cutoff. The cutoff energy in this approximation corresponds to $\sim$ 3 times the temperature of the Comptonizing cloud. This model, in the form $\mathrm{F(E)} \propto \mathrm{E}^{-\alpha} \times \exp(-\mathrm{E/kT})$, provided a better overall fit to the OSSE observation (χ^2 probability of 0.08) and, in particular, a more adequate description of the spectrum above $\sim$ 200 keV. For the September observation of GX 339$-$4 we obtained a power law spectral index of 0.88 $\pm$ 0.05 and a cutoff energy of (68 $\pm$ 2) keV; the normalization at 100 keV is (0.189 ± 0.001) photons cm^{-2} s^{-1} MeV^{-1}. While this result lends some support to the work of Haardt et al., we note that the OSSE data can be fit nearly as well with an optically thin thermal bremsstrahlung spectrum. This may not be surprising, since the functional forms of these two spectra differ only slightly in spectral index (α = 1 for bremsstrahlung).

Recent work by Ueda, Ebisawa, & Done (1994) indicated that the reflection model of Done et al. (1992) provided a good fit to X-ray spectra of GX 339$-$4 in its hard (low X-ray) state, obtained by GINGA during various observations. In this model, emission following a power law is partially Compton-reflected by cold, optically thick material in the disk. The emergent spectrum is a combination of the reflected spectrum and a portion of the power law that escapes directly without being reprocessed by the disk. While a simple power law provides a reasonable description of the continuum shape of the GINGA data below $\sim$7 keV, at higher X-ray energies it is harder than the observed spectrum; addition of the reflection

component evidently remedies this deficiency. When applied to the OSSE data, however, the reflection model failed to yield an acceptable fit: essentially none of the power law emission escapes directly along the line of sight, and the reflected portion of the model spectrum does not cut off with energy nearly as rapidly as the observed spectrum. The poor χ^2 of the fit (probability $< 10^{-15}$) confirmed what was evident upon inspection.

Compton reflection has also been discussed in the context of AGN observations. In a study concerning the spectra of Seyfert 1 galaxies, Madejski et al. (1994) and Zdziarski et al. (1994) invoked reflection for the case where the input power law includes an exponential cutoff. We applied their model to the GX 339−4 spectrum, adding a reflection component to the exponentially-cutoff power law model by processing the spectrum according to the angle-averaged model of Lightman & White (1988). The relative amount of reflection in this case is determined by the covering factor of the illuminating source as seen by the reflecting layer. The best fit was obtained with the maximum covering (4π steradians), but offers insignificant improvement (χ^2 probability of 0.11) over the unreflected spectrum. The best fit cutoff energy was (70 ± 3) keV, with a spectral index of 0.37 ± 0.06 (see Table 1).

Based upon fits to the OSSE data, we conclude that reflection of a pure power law spectrum can be ruled out for the September observation. The remaining models (Table 1) provide better descriptions of the observed spectrum, but we consider the Sunyaev-Titarchuk model to be only marginally acceptable. Because all are qualitatively similar in shape, we show only the results for optically thin Comptonization (i.e., power law with an exponential cutoff). The data and model from the combined, four-detector fits are displayed in Figure 3. The observed count spectrum was "unfolded" by multiplying the observed count data by the ratio of the best-fit model photon spectrum to the best-fit model count spectrum (the resulting photon spectrum was also rebinned in energy to improve the signal-to-noise in this figure). Integrating the unfolded spectrum from 50 to 400 keV gives a source luminosity of $\sim 2 \times 10^{37}$ ergs s^{-1} (at a distance of 4 kpc; cf. Makishima et al., and references therein), typical of the soft X-ray luminosity of sources like GX 339−4 in their high X-ray states.

Time-averaged spectra for each day of the September observation were also fit in order to investigate any possible daily variation in the parameters. No significant variability was found for any of the models; the day-to-day parameter values were nearly constant, and consistent with those derived from the spectrum averaged over the entire observation. This agrees with the nearly constant value of the daily count rates shown in Figure 2.

In the X-ray regime, the different states identified for GX 339−4 are clearly associated with changes in spectral shape, as well as fluence. Unfortunately, the relatively low signal-to-noise in the GX 339−4 spectrum obtained by OSSE in November makes it difficult to infer any change in shape relative to the spectrum observed in September. In fact, spectra

from the two observations are consistent with a drop in flux level only. At energies less than 150 keV, which comfortably includes the range where GX 339−4 was detected during both observations, the χ^2 probability that the ratio of the two spectra is constant is $\sim$ 60%. We fit the spectrum of the November observation with an exponentially-cutoff power law, but with the spectral index and cutoff energy fixed to their values determined from the fit to the September observation, and allowing only the amplitude to vary. As seen in Figure 4 and Table 1, the resulting fit is quite good (χ^2 probability of 97%), again consistent with a constant spectral shape. Of course, a change in spectral shape cannot be excluded on the basis of these data alone. Fits of a thermal bremsstrahlung model to the BATSE observations do show a variation in the derived temperature (Harmon et al. 1994), and observations with the SIGMA and ART-P instruments on the *Granat* satellite also indicate spectral evolution during this outburst of GX 339−4 (Grebenev et al. 1993). Further, the November OSSE observation can be fit equally well with a single power law model (see Table 1). The pure power law and cutoff power law differ significantly in shape only above about 150 keV, however, which is beyond the energy range of detection during the November observation. Since the relative weakness of the source during the November observation leads to somewhat ambiguous fitting results, inferring spectral evolution, aside from relative flux level, from just these two OSSE observations is not possible.

4. DISCUSSION

The supposition that the hard X-ray and gamma-ray spectrum of a binary X-ray source such as GX 339−4 is the signature of a black hole rests largely on its similarity to the spectra of the best black hole candidates, such as Cyg X-1 (Dolan et al. 1987; Miyamoto et al. 1992; Laurent et al. 1993), and even certain AGN (e.g., Haardt et al. 1993). To some extent, the appeal of the Sunyaev-Titarchuk spectrum is that it is developed from a physical, albeit idealized, model which may reasonably apply to the environs of an accreting black hole. Although this model provides only a marginal fit to the OSSE spectrum of GX 339−4, it cannot be concluded that the black-hole hypothesis is ruled out. Indeed, the Sunyaev-Titarchuk model does not fit the OSSE spectrum of Cyg X-1 either (Grabelsky et al. 1993). Grebenev et al. (1993) proposed that a similar deficiency of the model in describing SIGMA and ART-P observations of Cyg X-1 can be remedied by including the relativistic scattering cross-section and modeling a range of temperatures and optical depths. Alternatively, Haardt et al. (1993) have suggested that the high energy spectrum of Cyg X-1 is produced by thermal Comptonization in an optically *thin* accretion disk corona, and point out the approximate characterization of such a spectrum by a power law with an exponential cutoff. In this case, the cutoff energy is roughly 3 times that corresponding to the optically

thick corona which underlies the Sunyaev-Titarchuk model. Comparison of kT for these two models from our GX 339−4 fitting yields a factor of about two, in rough qualitative agreement with assumption of an optically thin corona.

An important clue to the nature of GX 339−4 might be provided by the relation between its X-ray and gamma-ray behaviors, in particular the correspondence between its X-ray states and gamma-ray outbursts. This point is especially relevant to the reflection models, which have been motivated primarily by the X-ray data. Two of the GINGA observations of GX 339−4 during its low X-ray state reported by Ueda et al. (1994) coincide with the OSSE observation made in September. We have already noted that the power law reflection model invoked to explain these low X-ray state of GX 339−4 fails to fit the OSSE data. However, the spectral index of $\sim$1.78 derived for the GINGA spectrum is quite close to that predicted for the low energy extension of the Sunyaev-Titarchuk fit to the OSSE spectrum. In Figure 5 we show three of the models used to fit the OSSE data, extrapolated to 5 keV; also displayed is the power law component of GINGA spectrum of 1991 September 11, which is a reasonable fit to the X-ray continuum spectrum below about 7 keV. Both the exponentially-cutoff power law and the Sunyaev-Titarchuk models appear to be fairly consistent with the slope and absolute flux level of the GINGA power law component. By contrast, the reflected optically thin Comptonization spectrum is inconsistent with the GINGA power law component, suggesting that it can be ruled out as a model. This was perhaps already indicated by the spectral index of 0.37, harder than any tail ever observed for GX 339−4 in its the low X-ray state (e.g., Nolan, et al. 1982; Makishima, et al. 1986). The apparent consistency between the GINGA and OSSE spectra provides strong evidence that the hard ($\gtrsim$ 10 keV) tail, characteristic of the low X-ray state of GX 339−4, connects to the low energy portion of its gamma-ray spectrum, and argues that the low X-ray state corresponds to gamma-ray outburst.

It is interesting to note that during the first OSSE observation, the total luminosity from 50–400 keV was $\sim 2.0 \times 10^{37}$ ergs s^{-1}. This is within a factor of 5 of the very high state X-ray luminosity reported by Miyamoto et al. (1991), and exceeds the low-state X-ray luminosity (cf. Tanaka & Lewin 1994, and references therein). During the second OSSE observation of GX 339−4, the 50–400 keV luminosity (from the unfolded photon spectrum in Figure 4) was $\sim 5 \times 10^{35}$ ergs s^{-1}, comparable to that in its low X-ray state. Thus the relative importance of gamma-ray production, at least during peak output, cannot be neglected in modeling of sources like GX 339−4.

Table 1: SPECTRAL MODEL PARAMETERS

Model	Norml.[a]	kT[b] (keV)	τ	α^c	χ^2 prob.
1991 September Observation...					
Sunyaev-Titarchuk	0.189 ± 0.001	37 ± 1	3.0 ± 0.1	1.9	4×10^{-3}
Power law $\times$ exp	0.189 ± 0.001	68 ± 2		0.88 ± 0.05	0.08
Thermal bremsstrahlung	0.188 ± 0.001	73 ± 1			0.07
Power law $\times$ exp + reflection[d]	0.190 ± 0.001	70 ± 3		0.37 ± 0.07	0.11
1991 November Observation...					
Power law $\times$ exp[e]	$(4.4 \pm 0.5) \times 10^{-3}$	68		0.88	0.97
Power law	$(3.9 \pm 0.5) \times 10^{-3}$			2.3 ± 0.3	0.97

Notes to table:

[a] Normalization (at 0.1 MeV): photons cm^{-2} s^{-1} MeV^{-1}.

[b] For the power law with an exponential cutoff the value in the table represents the cutoff energy, which is $\sim$ 3 times the temperature of the scattering cloud.

[c] α is derived from the model parameters for the Sunyaev-Titarchuk model (see text), but is a fitted parameter for the models with explicit power law components.

[d] The reflection component has been maximized in this fit; see text.

[e] The power law index and cutoff energy for the fit to the November observation were fixed at the values determined from the fit to the September observation.

REFERENCES

Cowley, A. P., Crampton, D., & Hutchings, J.B. 1987, AJ, 92, 195

Dolan, J. F., Crannell, C. J., Dennis, B. R., & Orwig, L. E. 1987, ApJ, 322, 324

Done, C., Mulchaey, J. S., Mushotzky, R. F., & Arnaud, K. A. 1992, ApJ, 395, 275

Fishman, G., Wilson, R., Meegan, C., Harmon, A., Brock, M., Paciesas, W., & Finger, M. 1991, *IAU Circular* No. 5327

Grabelsky, D. A., et al. 1993, in *Proc. Compton Symposium*, ed. M. Friedlander & N. Gehrels (New York: AIP), 345

Grebenev, S., et al. 1993 A&AS, 97, 281

Haardt, F., Done, C., Matt, G., & Fabian, A. C. 1993, ApJ, 411, L95

Harmon, B. A., et al. 1994, ApJ, 425, L17

Johnson, W. N., et al. 1993, ApJS, 86, 693

Laurent, P., et al. 1993, Adv. Space Res., 13, 139

Liang, E. P., & Nolan, P. L. 1984, Space Sci. Rev., 38, 353

Lightman, A. P., & White, T R. 1988, ApJ, 335, 57

Madejski, G. M., et al. 1994, ApJ, submitted

Makishima, K., Maejima, Y., Mitsuda, K., Bradt, H. V., Remillard, R. A., Tuohy, I. R., Hoshi, R., & Nakagawa, M. 1986, ApJ, 308, 653

Markert, T. H., Canizares, C. R., Clark, G. W., Lewin, W. H. G., Schnopper, H. W., & Sprott, G. F. 1973, ApJ, 184, L67

Miyamoto, S., Kimura, K, Kitamoto, S., Dotani, T., & Ebisawa, K. 1991, ApJ, 383, 784

Miyamoto, S., Kitamoto, S., Iga, S., Negoro, H., & Terada, K. 1992, ApJ, 391, L21

Nolan, P. L., Gruber, D. E., Knight F. K., Matteson, J. L., Peterson, L. E., Levine, A. M., Lewin, W. H. G., & Primini, F. A. 1982, ApJ, 262, 727

Pozdnyakov, L. A., Sobol, I. M., & Sunyaev, R. A. 1983, Astrophys. Space Phys. Rev., 2, 189

Purcell, W. R., Grabelsky, D. A., Ulmer, M. P., Johnson, W. N., Kinzer, R. L., Kurfess, J. D., Strickman, M. S., & Jung, G. V. 1993, in *Proc. Compton Symposium*, ed. M. Friedlander & N. Gehrels (New York: AIP), p. 107

Sunyaev, R. A., & Titarchuk, L. G. 1980, A&A, 86, 121

Tanaka, Y., & Lewin, W. H. G. 1994, in *X-ray Binaries*, ed. W.H.G Lewin, J. van Paradijs, & E.P.J van den Heuvel (Cambridge University Press), preprint

Ueda, Y., Ebisawa, K., & Done, C. 1994, PASJ, 46, 107

Zdziarski, A. A., Fabian, A. C., Nandra, K., Celotti, A., Rees, M. J., Done, C., & Madejski, G. M. 1994, in preparation

FIGURE CAPTIONS

Figure 1 – OSSE background-subtracted count spectra of GX 339−4 from both observation periods, and the estimated spectrum of the diffuse Galactic emission. The triangles show the spectrum from the 1991 September observation, summed over the entire one-week observation; the diamonds show the spectrum from the 1991 November observation. These two spectra represent the observed count rate from GX 339−4 plus a contribution due to diffuse emission from the Galactic plane. The crosses represent the estimated spectrum of the diffuse component in each of the observations of GX 339−4; this spectrum has been subtracted from the observed spectra prior to all subsequent analysis discussed in this paper. The data have been rebinned to improve the signal-to-noise in the figure. Note that the absence of upper limits allows visual comparison of the spectra only; see text.

Figure 2 – Average daily intensities during the 1991 September OSSE observation of GX 339−4. *(a)* 50–100 keV energy band; *(b)* 100–400 keV energy band; *(c)* (100–400 keV)/(50–100 keV) hardness ratio. The solid line in each figure is the corresponding quantity averaged over the observation period.

Figure 3 – Spectrum for the 1991 September OSSE observations of GX 339−4. The solid line in the upper plot shows the best-fit incident photon spectrum and the data points represent the unfolded (deconvolved) observed count spectrum; upper limits are 2σ. The lower plot shows the residuals (data − model). The photon model shown is a power law with an exponential cutoff. The data have been rebinned to improve the signal-to-noise in the figure. See §3 for a description of the fitting and unfolding process.

Figure 4 – Same as Figure 3, but for the 1991 November OSSE observations of GX 339−4. Note that for this observation the only free parameter of the model was the normalization amplitude at 100 keV; the power law index and the cutoff energy were fixed to their respective values from the fit to the September observation.

Figure 5 – Extrapolations of gamma-ray spectral models to 5 keV. The models shown are the power law with an exponential cutoff, Sunyaev-Titarchuk, and the exponentially-cutoff power law with reflection. The power law component of the fit to the GINGA data (Ueda et al. 1994) is plotted to 8 keV for comparison. The unfolded OSSE spectrum is also shown.

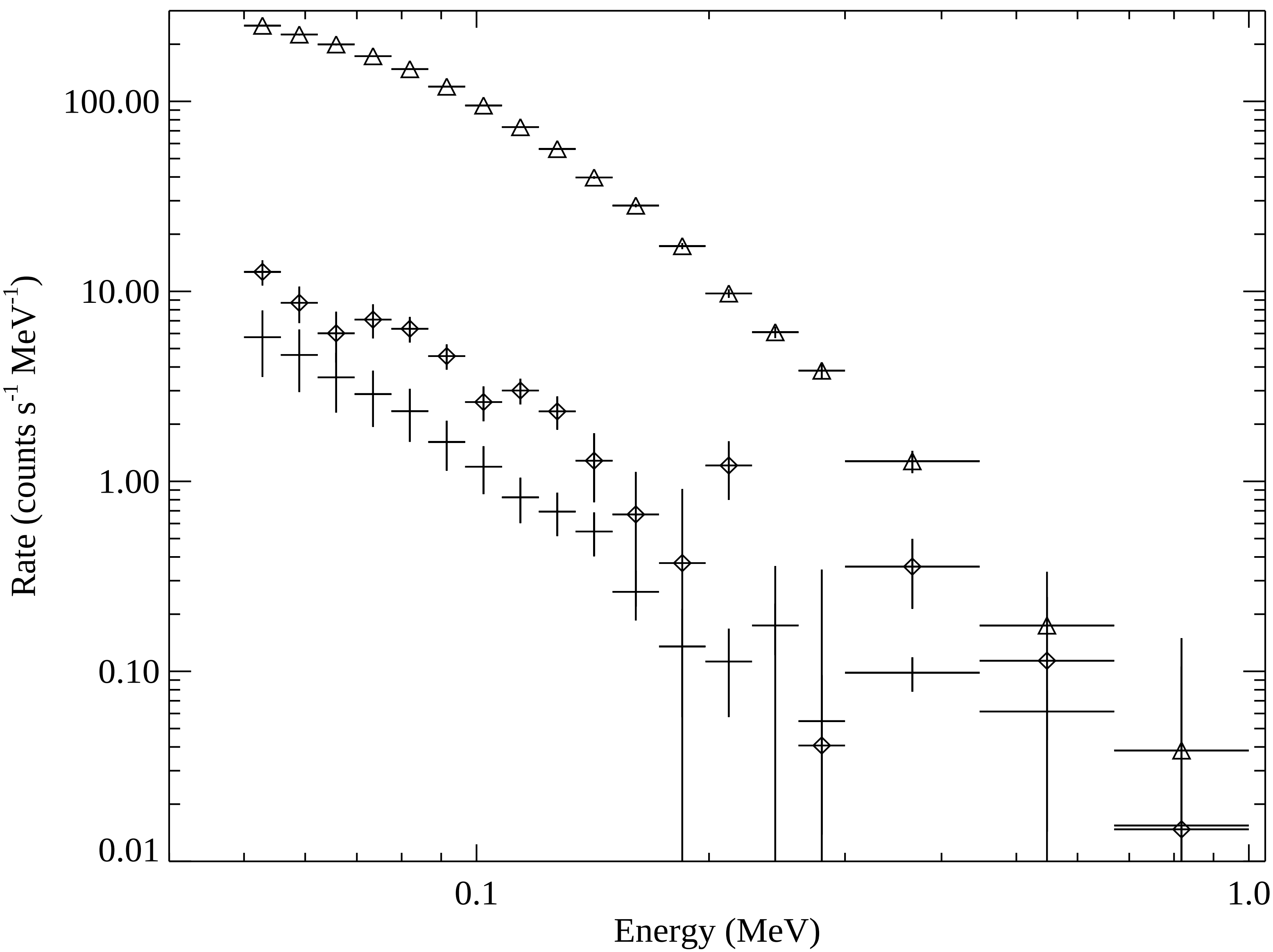

Rate (counts s^{-1} MeV^{-1})
100.00
10.00
1.00
0.10
0.01
0.1
1.0
Energy (MeV)

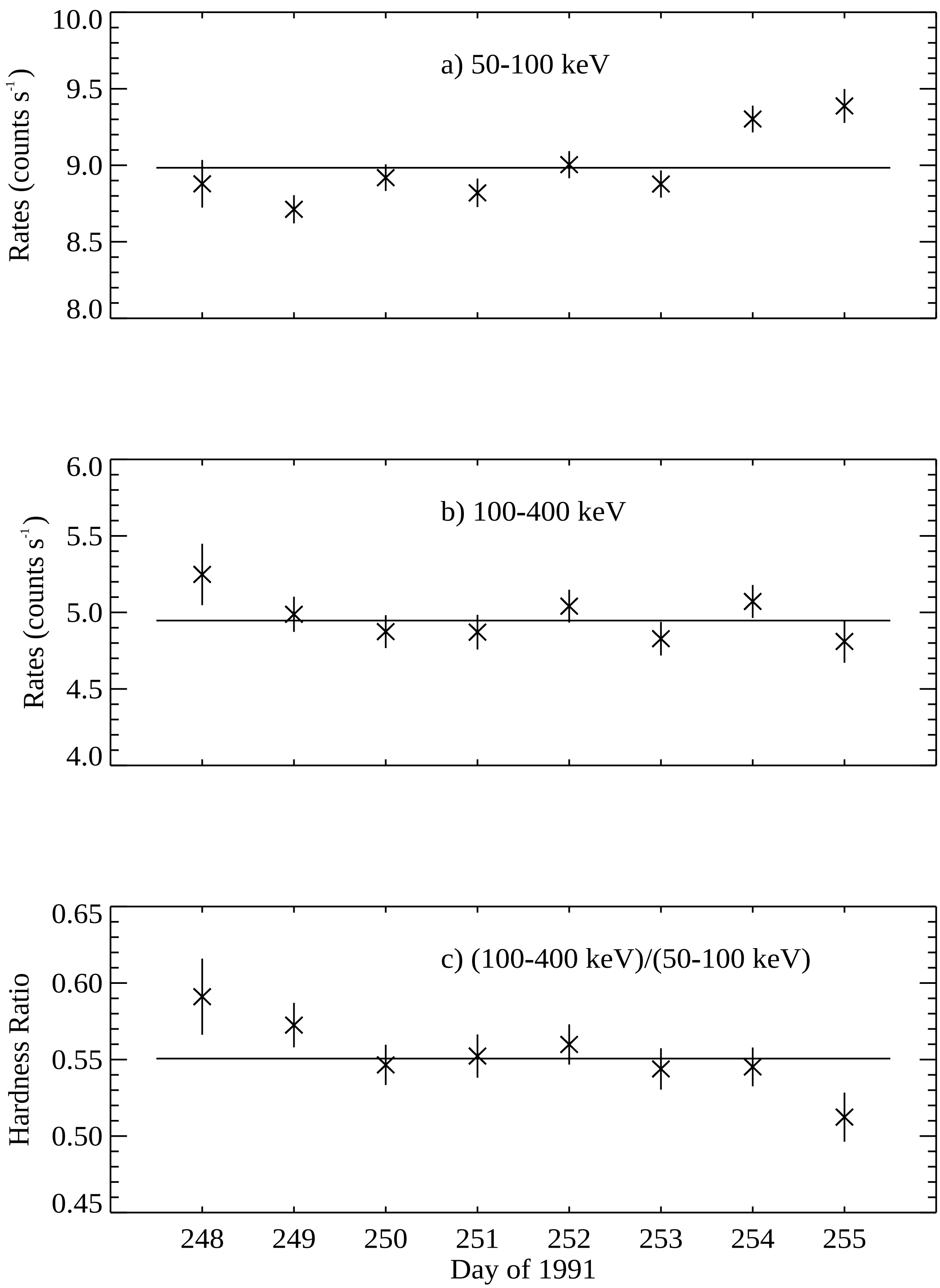
a) 50-100 keV
Rates (counts s^{-1})
10.0
9.5
9.0
8.5
8.0
b) 100-400 keV
Rates (counts s^{-1})
6.0
5.5
5.0
4.5
4.0
c) (100-400 keV)/(50-100 keV)
Hardness Ratio
0.65
0.60
0.55
0.50
0.45
248
249
250
251
252
253
254
255
Day of 1991

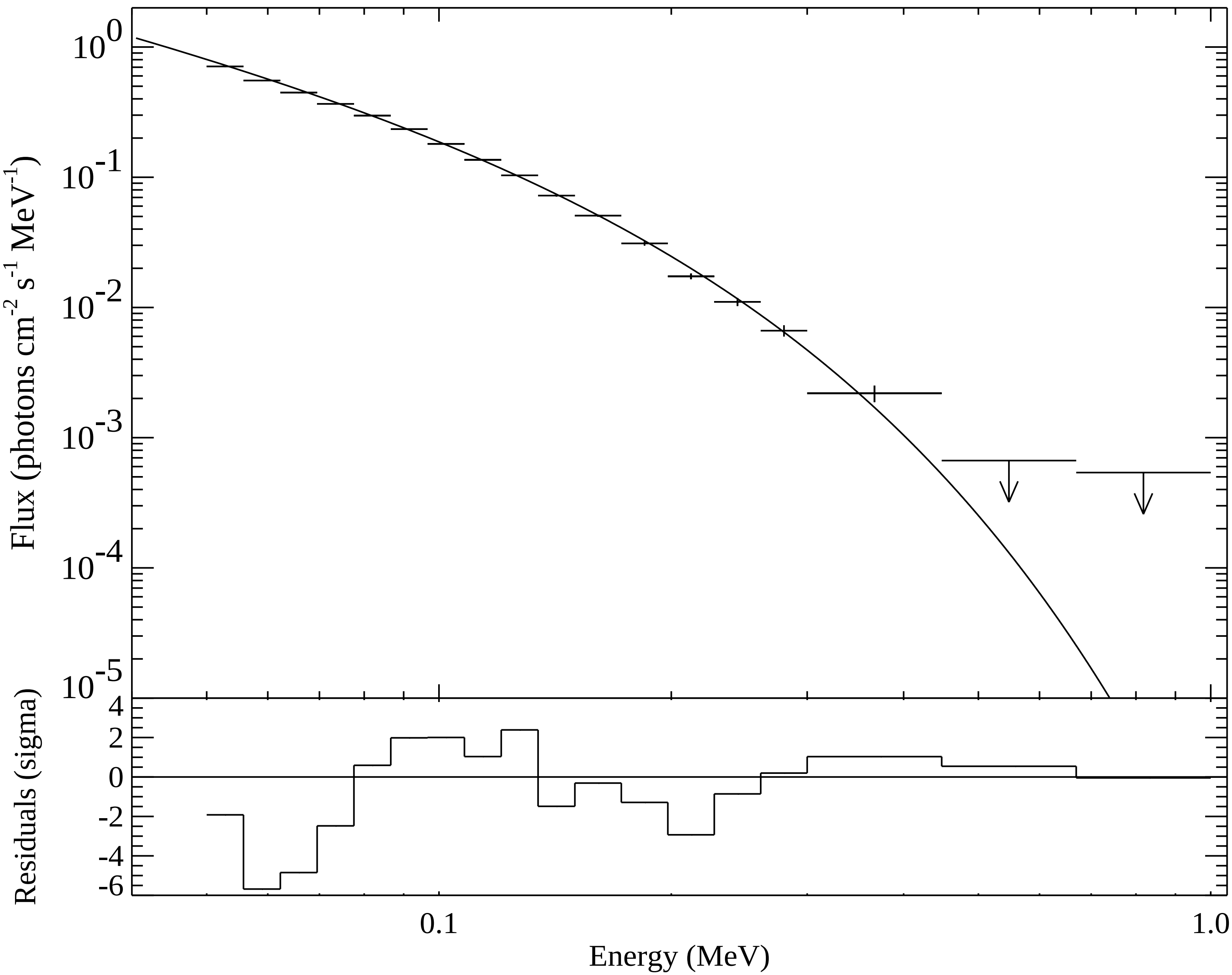

Flux (photons cm^{-2} s^{-1} MeV^{-1})
10^{0}
10^{-1}
10^{-2}
10^{-3}
10^{-4}
10^{-5}
Residuals (sigma)
4
2
0
-2
-4
-6
0.1
1.0
Energy (MeV)

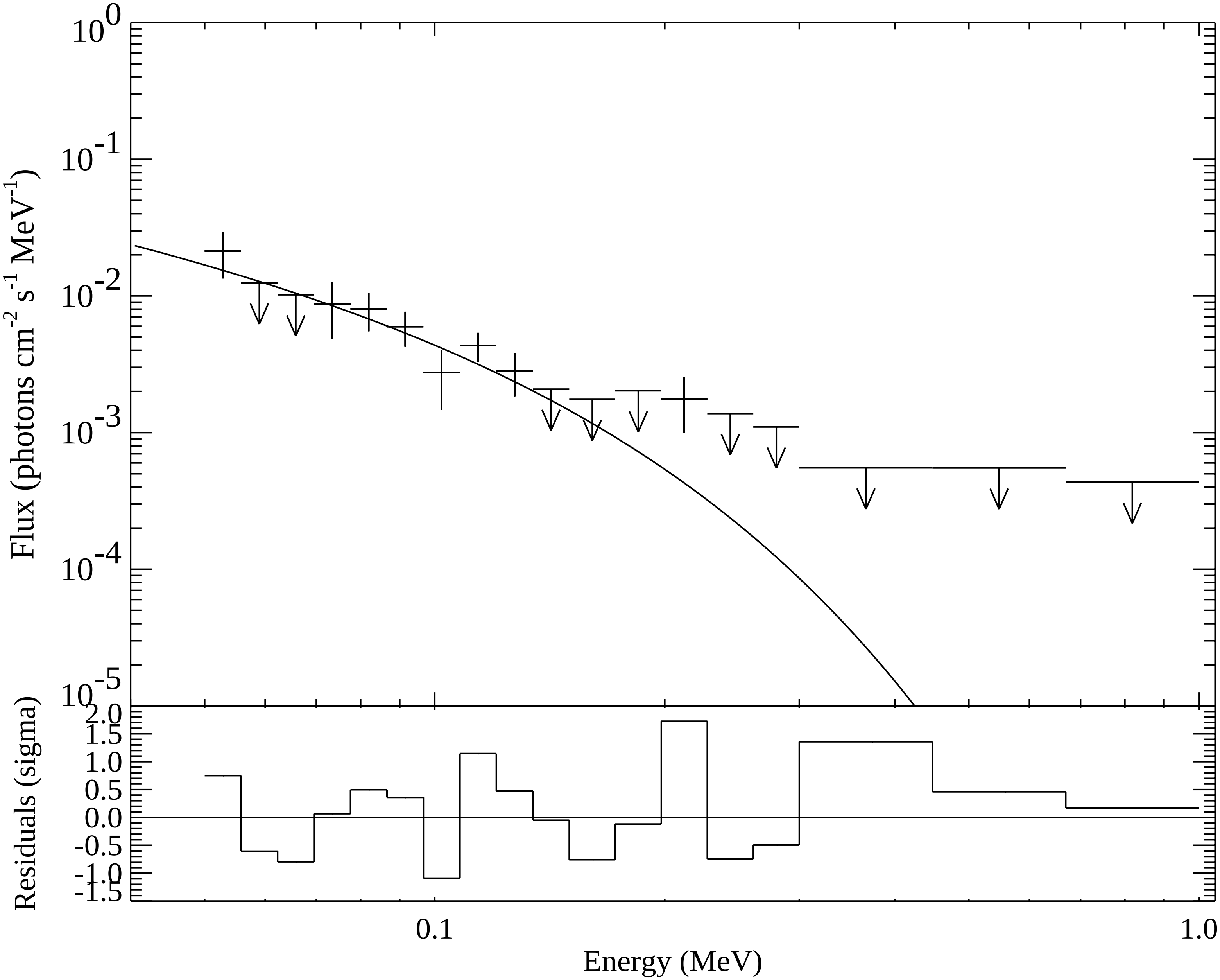

10^0
10^{-1}
10^{-2}
10^{-3}
10^{-4}
10^{-5}
Flux (photons cm^{-2} s^{-1} MeV^{-1})
2.0
1.5
1.0
0.5
0.0
-0.5
-1.0
-1.5
Residuals (sigma)
0.1
1.0
Energy (MeV)

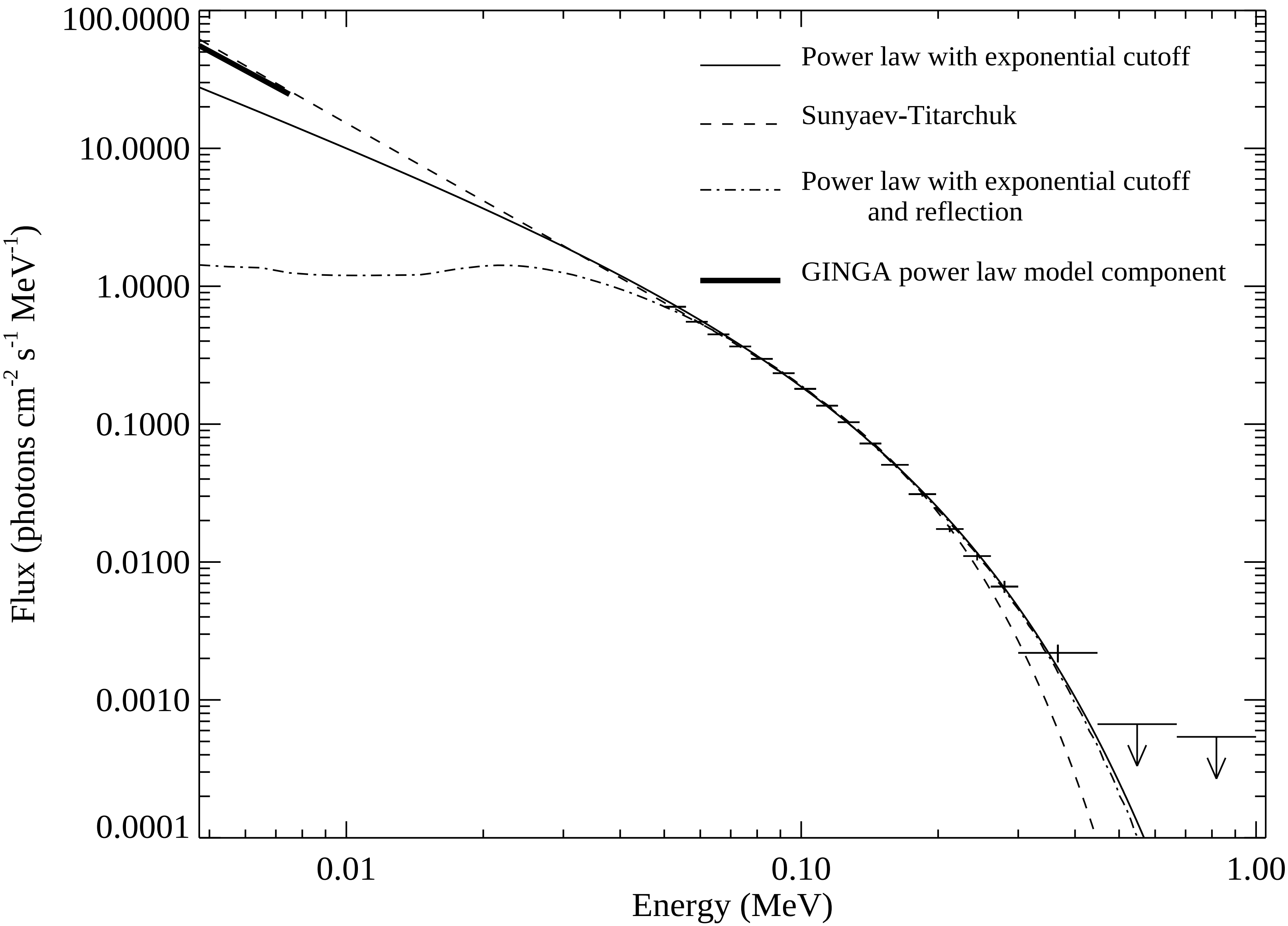

Power law with exponential cutoff
Sunyaev-Titarchuk
Power law with exponential cutoff and reflection
GINGA power law model component
Flux (photons cm^{-2} s^{-1} MeV^{-1})
100.0000
10.0000
1.0000
0.1000
0.0100
0.0010
0.0001
0.01
0.10
1.00
Energy (MeV)